Fundamentals of Bubble Formation during Coagulation and Sedimentation Processes

Paolo Scardina[1] and Marc Edwards[2]

Abstract: Conventional coagulation and sedimentation processes can be significantly disrupted by gas bubbles, attaching to, and then floating coagulant floc. This study sought to understand the fundamental factors that lead to bubble formation and corresponding floating floc during coagulation and sedimentation. Gas bubbles (causing the floating floc) can form whenever the total dissolved gas pressure exceeds the local solution pressure, which can occur at localized minimum pressures during rapid mixing at high fluid velocities. Very high rate rapid mixers can cause bubble formation and floating floc even in waters undersaturated with dissolved gas. The formation and stability of floating floc are dependent on the local solution pressure, amount and type of dissolved gas supersaturation, temperature, length of rapid mixing, surface chemistry of the mixing paddle, floc, and attachment forces.

DOI: 10.1061/(ASCE)0733-9372(2006)132:6(575)

CE Database subject headings: Bubbles; Coagulation; Sedimentation; Gas; Water treatment plants; Flocculation.

Introduction

Gas bubbles suspended in solution can attach to coagulated floc particles creating "floating" or "rising" floc in conventional drinking water treatment plants (Fig. 1). Floating floc reduces settling efficiency during sedimentation. Subsequent floc carry-over can overload filters, such that in extreme events, the filter can become the only physical barrier for pathogen and particle removal. Even bubbles detectable only by close visual inspection (bubble diameters $\leq$0.5 mm) can potentially cause floating floc. For example, given that the density of floc particles (aluminum or iron hydroxide plus turbidity) is often only slightly greater than that of water (e.g., 1.1 g/mL floc), consideration of particle buoyancy indicates that settling of 1 g of floc would be prevented if 0.03 mL of bubbles were attached.

Gas bubbles can form in solution whenever the total dissolved gas (TDG) pressure exceeds the local solution pressure (Scardina and Edwards 2001). Under such conditions, the water is considered supersaturated with dissolved gas. Since dissolved gas supersaturation can result from mechanical, chemical, or microbial processes (Scardina and Edwards 2002), plants can experience daily, seasonal, or diurnal events that can lead to bubble formation and subsequent floating floc.

Utilities afflicted with these problems often make futile attempts to improve settling of the floating floc, and in other cases utility personnel do not even know how to recognize bubbles as the problem. A better fundamental understanding is necessary to educate treatment plant operators and managers as to the consequences of bubble formation with respect to plant operation. Root causes and possible solutions to these problems need to be clearly identified.

This study investigated the initial formation and then stability of floating floc during conventional coagulation-sedimentation processes. Various design and operational parameters of a coagulation system and also intrinsic properties of the raw water solution were varied in benchscale laboratory experiments. The overall development of floating floc was observed, with the goal of determining simple procedures to mitigate this problem.

Materials and Methods

Benchscale laboratory coagulation experiments were conducted with a standard jar tester (maximum mixing speed=160 rpm) using 1 L square jars (9 cm side length). The paddles had a dimension of $7.5 \times 2.5 \times 0.1$ cm and were positioned in the middle of the jars. Handheld devices (drills) were used in some experiments to rapid mix at higher revolutions per minute as measured by a tachometer. When using a drill, the top of the jars had to be covered to prevent water loss.

For each experiment, 0.85 g of $NaNO_3$ and 1.0 mL of a 0.52 M as SO_4^{-2} Na_2SO_4 stock solution were added to the jars prior to filling to 1 L with distilled-deionized source water. No additional turbidity particles were added to these solutions, which were then dosed with either a 0.13 M as Al liquid stock solution of alum $[Al_2(SO_4)_3 \cdot 18H_2O]$ or 0.27 M as Fe $FeCl_3 \cdot 6H_2O$ coagulant. Since coagulant flocs formed quickly at a dose of 14.5 mg/L as Al, this alum dosage was used throughout most of the study. At the start of rapid mixing (time, $t=0$), the coagulant was added along with 1 M sodium hydroxide (NaOH). The two chemicals were dosed at opposing corners of each jar to produce a final coagulation pH of 6.0±0.2. The ionic strength of most alum coagulated waters with dissolved nitrogen supersaturation was 0.016 M.

For all experiments, the waters were rapid mixed between 0 and 600 s depending on the experiment, flocculated for 30 min, and allowed to settle for 30 min. The rapid mix and flocculation

[1]Post-Doc, Virginia Tech, 418 Durham Hall, Blacksburg, VA 24061.
[2]Charles P. Lunsford Professor, Virginia Tech, 407 Durham Hall, Blacksburg, VA 24061.

Note. Discussion open until November 1, 2006. Separate discussions must be submitted for individual papers. To extend the closing date by one month, a written request must be filed with the ASCE Managing Editor. The manuscript for this paper was submitted for review and possible publication on June 13, 2005; approved on October 25, 2005. This paper is part of the ***Journal of Environmental Engineering***, Vol. 132, No. 6, June 1, 2006. ©ASCE, ISSN 0733-9372/2006/6-575–585/$25.00.

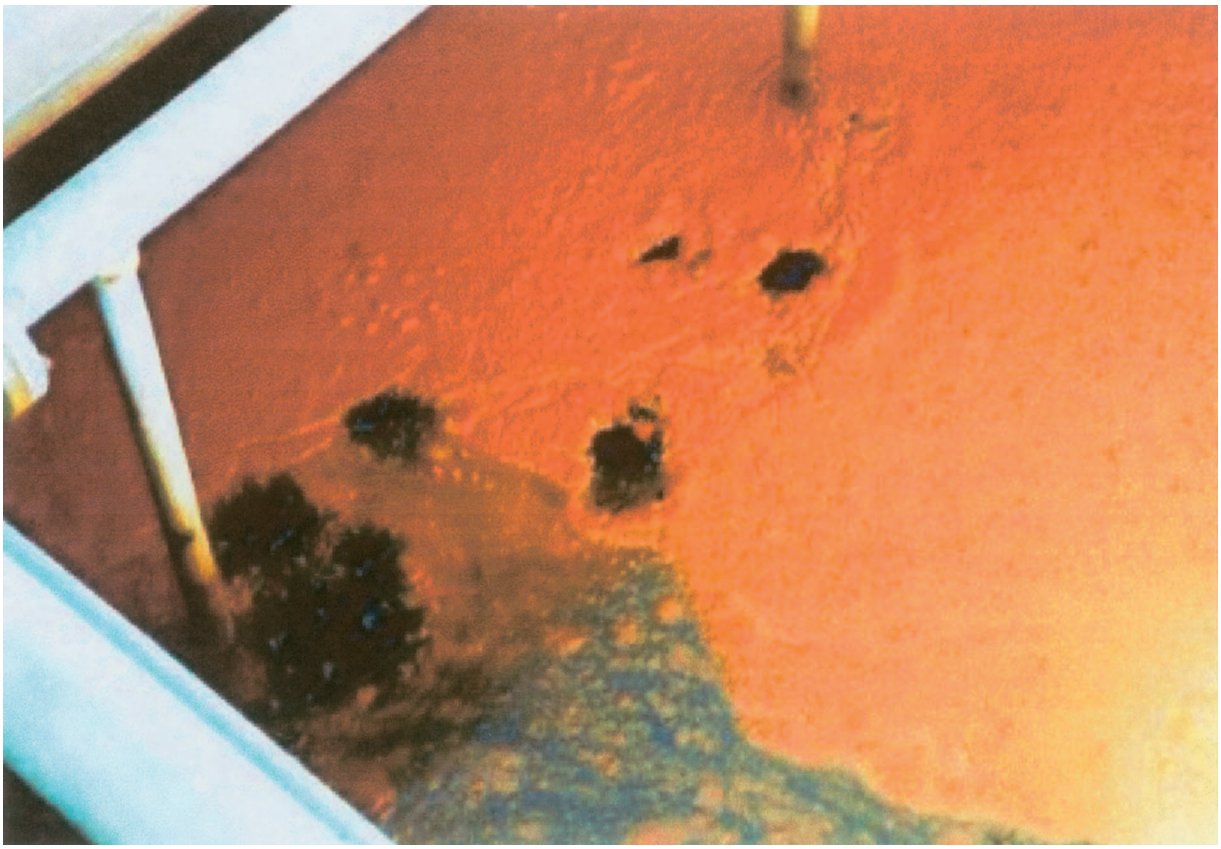

Fig. 1. (Color) Floating floc (iron coagulant) collected above a filter at a water treatment plant

rates (revolutions per minute, rpm) were varied as specified for each experiment, and mixing intensities were converted into mean velocity gradients (G values) using equations outlined in Droste (1997).

The final settled turbidity, pH, TDG, and volume of floating floc were measured at the end of 30 min of sedimentation. Final settled turbidity samples were drawn from the middle of the jar and measured with a HACH 2100 N benchtop turbidimeter. It is understood that suspended gas bubbles measure as turbidity (HACH 1997; Scardina 2004; Edwards et al. 2004), and since samples were not degassed prior to measurement, gas bubbles may have contributed to the solution turbidity. However, it is generally believed that their contribution was slight since 5 min was allowed for bubbles to rise from mixed collected sample solutions.

In this study, the driving force for gas bubble formation was created by supersaturating the water with dissolved gas (Scardina and Edwards 2001). A total dissolved gas probe (TDGP) manufactured by Sweeney Aquametrics was used to measure the TDG pressure of the solution. Most data are reported as gauge pressures (±0.002 atm) referenced to the local barometric pressure which is also measured by the TDGP (±0.002 atm). For example, a water at equilibrium with 1 atm barometric pressure (100% saturation) would have a TDG of 0 atm gauge pressure or 1 atm absolute pressure. Any dissolved gas supersaturation or undersaturation would have a positive or negative gauge pressure, respectively. The TDGP also corrects the TDG pressure based upon the solution temperature, which is also measured by the TDGP (±0.1 °C).

Since the distilled and deionized source water was initially undersaturated with dissolved gas (TDG between −0.013 and −0.066 atm gauge pressure), the source water was placed in an enclosed chamber where the headspace above the water was pressurized with nitrogen gas at 0.20–0.35 atm gauge pressure. The water in this pressurized chamber was stirred to increase transfer of gas into solution. Initial TDG measurements indicated that 0.07 atm gauge pressure was lost during transfer from the pressurized chamber to the coagulation jars, so the water was pressurized inside the chamber to 0.27 atm gauge pressure to give an initial supersaturation of 0.20 atm gauge pressure within the coagulant jars at the start of all experiments, unless otherwise indicated. Unless otherwise noted, experiments were conducted with nitrogen supersaturation.

In some experiments, the solutions were supersaturated (0.20 atm total gauge pressure) with dissolved carbon dioxide. In these tests, the source water was initially aerated to saturation (0.00 atm gauge pressure) using air, followed by the addition of sodium bicarbonate, and the pH was then acidified to 6.0 converting the bicarbonate alkalinity to dissolved carbon dioxide. Initial measurements determined that 1.50 g/L $NaHCO_3$ produced solutions that were supersaturated with dissolved gas at 0.20 atm gauge pressure after acidification. The final ionic strength of these solutions was 0.029 M.

Results and Discussion

The fundamental factors that influence bubble formation and floating floc are first introduced, followed by a qualitative description of jar test observations. A series of jar tests are then presented that confirm key hypotheses. Finally, some additional

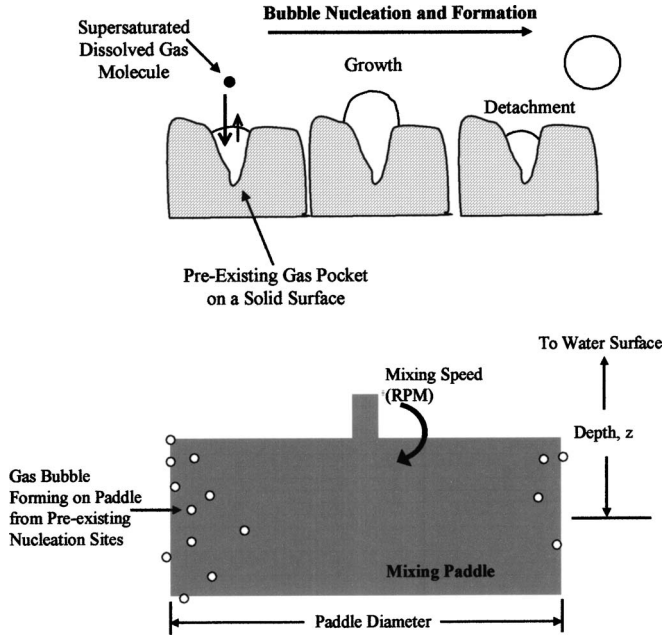

Fig. 2. Gas bubble formation by heterogeneous nucleation: (top) schematic and (bottom) on the mixing paddle (paddle rotation was clockwise; some bubbles are also present on the wall of the jar)

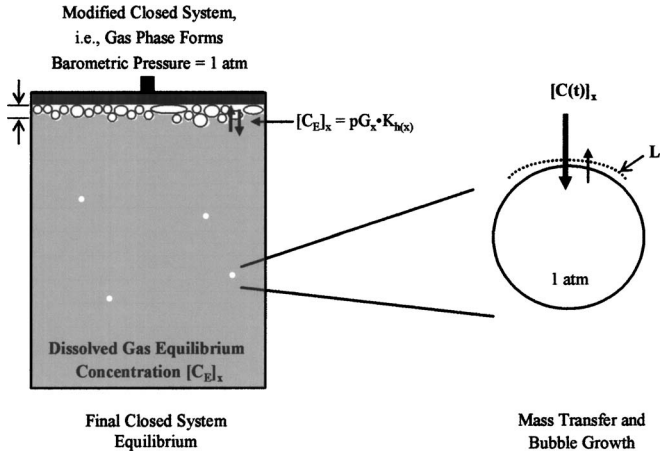

Fig. 3. Gas bubbles form until equilibrium is reached for each dissolved gas (x) between water and (left) the local atmosphere created by the bubbles, and (right) conceptualization of gas transfer kinetics as system approaches equilibrium via bubble formation

considerations with respect to coagulation systems and floating floc are discussed.

Fundamental Background on Bubble Formation during Coagulation and Mixing

Bubbles at Equilibrium with Dissolved Gas

A gas bubble can form in solution whenever the TDG pressure exceeds the local solution pressure, i.e., dissolved gas supersaturation (Scardina and Edwards 2001). Since most conventional treatment plants function essentially as closed systems with respect to the atmosphere in terms of gas transfer across the liquid-atmosphere surface (Letterman and Shankar 1996), bubble formation can be the main mechanism to alleviating dissolved gas supersaturation. Given the initial dissolved gas supersaturation in most of these experiments (0.20 atm gauge pressure), the bubbles originated via heterogeneous nucleation from preexisting gas pockets located on solid surfaces, such as the mixing paddle or side of the jar (Fig. 2) (Scardina and Edwards 2001; Harvey 1975). The number and type of nucleation sites are related to the roughness and hydrophobicity of the surfaces (Ryan and Hemmingsen 1998), and surfactants can either promote or reduce bubble formation (Hilton et al. 1993).

Conceptually, a modified closed system analysis is useful for predicting gas transfer and bubble formation in treatment plants. Considering water initially (time, $t=0$) supersaturated with dissolved gas at a concentration $[C(t)]_x$ for each individual gas species x, bubbles can continue forming or growing until the system reaches equilibrium with the newly formed gas phase (Fig. 3) and not the atmosphere (closed system). For conditions typically present in water treatment (dilute solutions with respect to atmospheric gases), Henry's gas law is applicable rather than Raoult's law (Betterton 1992) for dissolved gas equilibrium of gas species x

$$[C_E]_x = pG_x K_{h(x)} \tag{1}$$

where $[C_E]_x$=equilibrium dissolved gas concentration; pG_x=partial pressure in the gas phase; and $K_{h(x)}$=Henry's gas law constant which is temperature dependent. Equilibrium conditions would, therefore, be a function of the amount of initial dissolved gas supersaturation, local pressure, dissolved gas type, and solution temperature.

A gas bubble equilibrium model based upon this modified closed system assumption (Scardina and Edwards 2001) can be used to estimate the volume of bubbles formed (mL/L) and the equilibrium dissolved gas concentration $[C_E]_x$ for solutions initially supersaturated with dissolved gas. The composition of the gas bubble includes any dissolved gases that transferred to the gas phase plus water vapor, assuming that the pressure within the bubble equals the barometric pressure (Fig. 3). For example, consider two types of waters at 20°C both starting with 0.20 atm gauge pressure dissolved gas supersaturation (Table 1). One water is supersaturated with 1.20 atm absolute pressure dissolved nitrogen. The second water is initially aerated with 79% nitrogen and 21% oxygen at 1.00 atm absolute pressure, and an additional 0.20 atm absolute pressure dissolved carbon dioxide is formed by addition of $NaHCO_3$ and acid. Henry's law can be used to convert partial pressures to concentration units [Eq. (1)].

The difference between the initial known concentration $[C(t)]_x$ and the predicted equilibrium concentration $[C_E]_x$ [computed by the Scardina and Edwards (2001) modified closed system model] of each individual dissolved gas (x) would be the amount transferred to the gas bubbles per 1 L solution. In the system supersaturated at 0.20 atm gauge pressure nitrogen, the modified closed system model predicts that 1.6×10^{-4} moles of nitrogen would transfer to the gas bubbles, and including the additional contribution of water vapor, the total bubble volume formed would be 3.91 mL (Table 1). In the other water with 0.20 atm gauge pressure carbon dioxide supersaturation, only 0.5×10^{-4} moles of carbon dioxide are predicted to transfer to gas bubbles (Table 1), yet nitrogen and oxygen would also transfer to the gas bubbles until their respective equilibrium is reached (Scardina and Edwards 2001). Thus, including all the gases in this newly formed gas bubble, a larger total bubble volume 5.53 mL should form in this water at equilibrium (Table 1).

Table 1. Illustrative Calculation of Gas Type and Temperature Relative to Bubble Formation

Type of dissolved gas supersaturation		Initial TDG (atm, absolute)	Temperature (°C)	Initial dissolved gas concentration $[C(t)]_x$ (M)	Equilibrium dissolved gas concentration[a] $[C_E]_x$ (M)	Initial driving force $[C(t)-C_E]_x$ (M)	Diffusion constant[b] (D_L) (cm^2/s)	Equilibrium bubble formation[a] (mL/L)	Initial mass transfer rate[c] (nmol/h)	Measured floating floc[d] (mL/L)
Nitrogen		1.20	20	8.34×10^{-4}	6.79×10^{-4}	1.55×10^{-4}	1.806×10^{-5}	3.91	10.0	14.5
Carbon dioxide[e]	CO_2	0.20		78.68×10^{-4}	78.23×10^{-4}	0.45×10^{-4}	1.311×10^{-5}			
	N_2	0.79	20	5.49×10^{-4}	4.15×10^{-4}	1.34×10^{-4}	1.806×10^{-5}	5.53	13.3	0
	O_2	0.21		2.91×10^{-4}	2.50×10^{-4}	0.41×10^{-4}	1.643×10^{-5}			
Carbon dioxide[e]	CO_2	0.10		39.41×10^{-4}	39.30×10^{-4}	0.11×10^{-4}	1.311×10^{-5}			
	N_2	0.79	20	5.49×10^{-4}	4.74×10^{-4}	0.75×10^{-4}	1.806×10^{-5}	2.70	6.6	1.1
	O_2	0.21		2.91×10^{-4}	2.70×10^{-4}	0.21×10^{-4}	1.643×10^{-5}			
Nitrogen and	N_2	1.10	20	7.65×10^{-4}	6.10×10^{-4}	1.55×10^{-4}	1.806×10^{-5}	4.35	10.9	0
carbon dioxide[e]	CO_2	0.10		39.41×10^{-4}	39.23×10^{-4}	0.18×10^{-4}	1.1311×10^{-5}			
Nitrogen		1.20	10	10.02×10^{-4}	8.25×10^{-4}	1.77×10^{-4}	0.690×10^{-5}	4.22	4.4	5.2

[a]Calculated with the Modified Closed System Model (Scardina and Edwards 2001).

[b]Diffusion constants calculated from Hayduk and Laudie (1974) and converted to appropriate temperature using Selleck et al. (1988).

[c]Diffusion layer thickness (L=0.1 mm) and surface area (SA=1 mm^2) assumed to be constant for initial conditions.

[d]Waters rapid mixed at 80 rpm (G=120 s^{-1}) for 60 s and flocculated at 5 rpm (G=2 s^{-1}).

[e]Solution initially supersaturated by acidifying carbonate system to pH of 6.0.

These examples illustrate the importance of the initial system conditions in relation to total bubble formation. A similar comparison of dissolved nitrogen supersaturation (0.20 atm gauge pressure) at 10 and 20°C shows that colder solutions also form more gas bubble volume when equilibrium is reached (Table 1).

Mass Transfer of Dissolved Gas to Gas Bubbles

In the benchscale experiments to be discussed later, waters initially supersaturated with dissolved gas did not reach equilibrium in a time scale of hours, as indicated by TDG measurements on settled waters. Thus, the rate of mass transfer from the dissolved phase to the gaseous phase is also a controlling factor in bubble formation. The rate of mass transfer $(dM/dt)_x$ in units of nanomoles/h would be a function of the system conditions (Fig. 3)

$$\text{mass transfer} = (dM/dt)_x = K_L \text{SA}[C(t) - C_E]_x \tag{2}$$

The mass transfer parameter K_L (cm/s)=liquid diffusion constant D_L (cm^2/s) divided by the diffusion layer thickness L (mm) (Fig. 3). Dissolved gases transfer across a bubble or preexisting gas pocket surface area SA (mm^2). The driving force of bubble formation is the difference between the actual (supersaturated) dissolved gas concentration and the concentration at equilibrium $[C(t)-C_E]_x(M)$ for each particular gas. For illustrative calculations of relative mass transfer rates, the diffusion layer thickness L and surface area SA were assumed to be 0.1 mm and 1 mm^2, respectively.

The diffusion constant (D_L) varies for each dissolved gas (Hayduk and Laudie 1974) and is a function of the solution temperature (Selleck et al. 1988). The diffusion constant can have significant effects on the rate of bubble formation. For example, the driving force is greater for a water at 10°C and 1.20 atm absolute pressure dissolved nitrogen, than for a water with the same TDG at 20°C (Table 1). However, lower diffusion in the colder solution causes a 56% reduction in the overall rate of mass transfer, which might be expected to produce slower bubble formation initially (Table 1). Yet, if this water was given sufficient time to reach equilibrium, then the total bubble formation would be about 8% greater in the colder solution (Table 1).

The concentration driving force $[C(t)-C_E]_x$ also affects mass transfer [Eq. (2)]. Considering the water supersaturated to 0.20 atm gauge pressure with nitrogen compared to a water supersaturated to 0.20 atm gauge pressure with carbon dioxide, a 33% greater mass transfer rate would be expected in the water supersaturated with carbon dioxide (Table 1). Mass transfer, like equilibrium, is a fundamental property controlling bubble phenomena and the development of floating floc. The rate of mass transfer is also dependent on chemistry of the water.

Location of Gas Bubble Nucleation

The mechanism by which bubbles form in water treatment plants is heterogeneous nucleation (Scardina and Edwards 2001; Harvey 1975). Bubbles could form on the mixing paddle, since this is often a location of minimum pressure in the system (Fig. 2). As the paddle rotates through the fluid at a high rate, the higher velocity would reduce the local solution pressure, which has been described by the energy equation for similar conditions of flow within pipes

$$P/\lambda + V^2/(2g) + z = \text{constant} \tag{3}$$

Due to the nonideal turbulent mixing environment, the energy equation [Eq. (3)] is not a perfect description of the local solution pressure (P) in a jar test, but it can illustrate key concepts (Robertson and Crowe 1993). The velocity (V) was assumed to be the product of the mixing speed (rpm) and the circumference made by the rotating paddle at a particular depth (z) [Fig. 2 (bottom)]. Even if bubbles cannot form on a paddle at rest because the local solution pressure is greater than the TDG pressure, mixing can reduce the local solution pressure to conditions favorable for bubble formation (TDG > local pressure) (Fig. 4).

Although the actual local solution pressure at the paddle surface is nearly impossible to calculate or measure directly, a manometer tube positioned on each side of the mixing paddle can provide another estimate of the local pressure (Fig. 5). A lower local pressure during mixing would decrease the height of water in the manometer tube, as monitored with gradations marked on the shaft (Fig. 5). Using this device, it was shown that the local solution pressure during rapid mixing was lower than the nonmix-

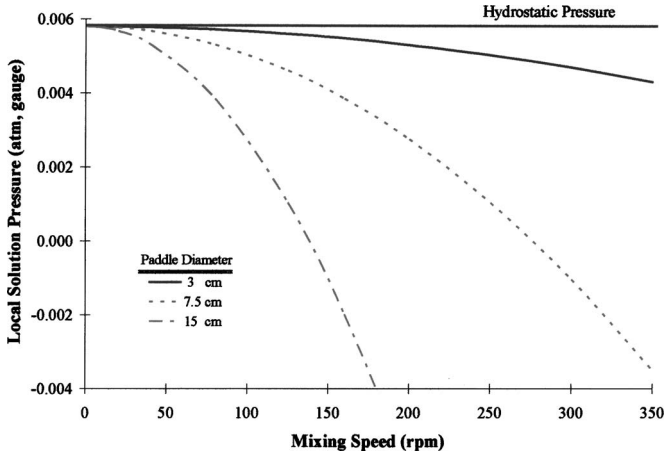

Fig. 4. Calculated local solution pressure at the outermost tip of the paddle estimated for the jar tester at a depth of 6.0 cm using the energy equation [Eq. (3)]

ing hydrostatic pressure (Fig. 6), and the local solution pressure rapidly decreased at higher mixing speeds [Fig. 6 (bottom)]. At mixing speeds greater than 305 rpm, all of the water in the manometer tube was completely evacuated, suggesting pressures at the paddle less than the barometric pressure (negative local gauge pressures) [Fig. 6 (bottom)].

For a given mixing speed, the pressure was consistently lower on the reverse side of the paddle [Fig. 6 (top)]. When a paddle moves through a solution, the fluid streamlines separate and break around the paddle, creating a very turbulent area on the reverse side of the paddle known as a wake (Birkhoff 1957; Van't Riet and Smith 1975). At very high mixing rates, the wakes can also become gaseous cavities (Van't Birkhoff 1957). This was in agreement with the fact that bubble formation was observed to be more prominent on the back of the paddle.

The manometer data was actually fairly well approximated by the energy equation [Eq. (3)] (Fig. 6). Given the formation of

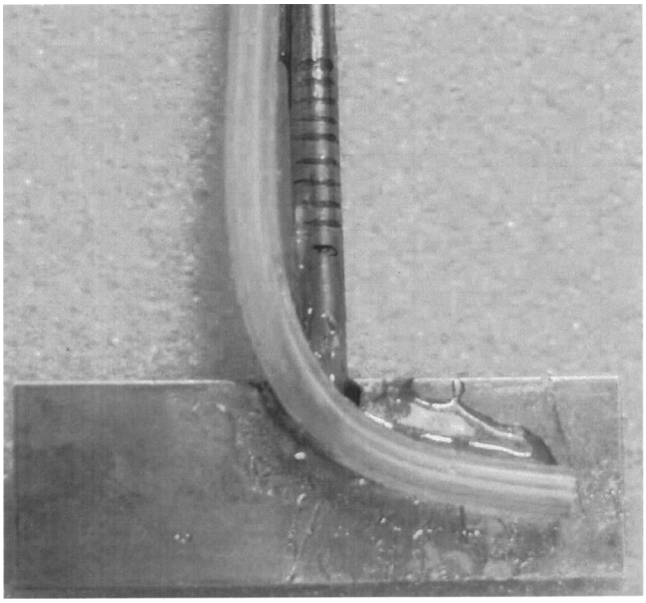

Fig. 5. Crude manometer tube affixed to mixing paddle

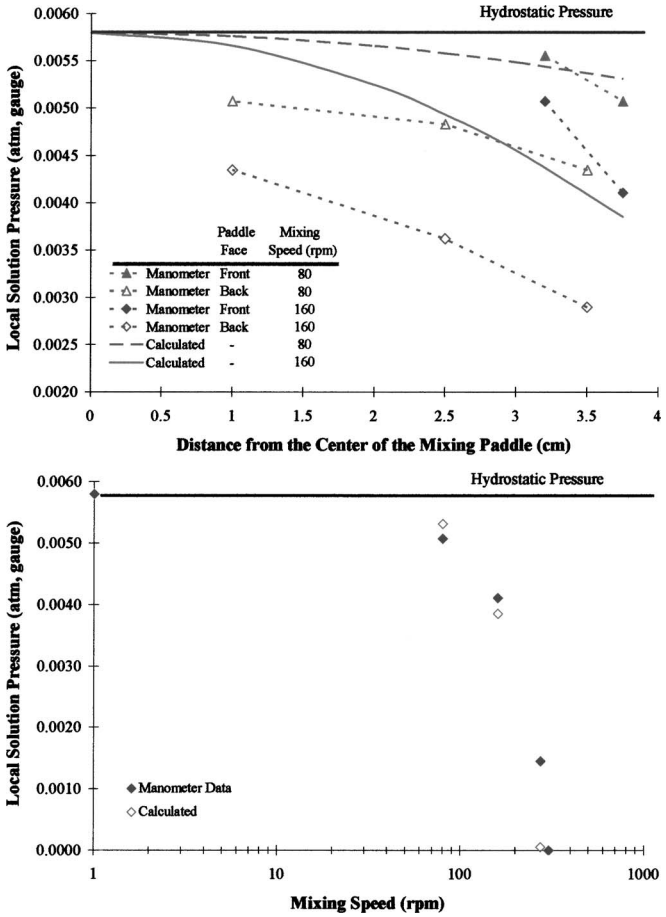

Fig. 6. Change in local solution pressure while mixing for the front and back of the paddle face (top) and front face as a function of different mixing speeds (botom). Pressure was measured with a manometer on the paddle (Fig. 5), and the energy equation [Eq. (3)] was used to calculate the local solution pressure.

wakes, though, the measured local solution pressure on the backside of the paddle was on average 25% less than that predicted by the energy equation in these experiments.

Generalized Observations Related to Bubble Phenomenon in Jar Tests

The formation of floating floc during jar tests was reproducible in benchscale laboratory experiments. Floating floc in most experiments was associated with reduced particle removal and settling efficiency, and the final turbidity of water after settling was sometimes higher in the solutions with floating floc than waters with no floating floc (Fig. 7). However, it was evident that final settled turbidity was not a good indicator of treatment disruptions caused by gas bubbles, since so much of the floc was floating (Fig. 7). To quantify the floating floc, a new parameter was developed where the diameter and thickness of the floc floating at the water surface was measured to estimate the total volume of floating floc (mL/L) (Fig. 8). This estimation was reproducible between ±1 mL or ±10%, whichever is greater.

After filling the coagulant jars with water supersaturated with dissolved gas, many minute bubbles could be seen in solution upon close inspection originating from nucleation sites on the bottom and sides of the jars. Without mixing, these bubbles would float to the water surface in about one minute. Some of these

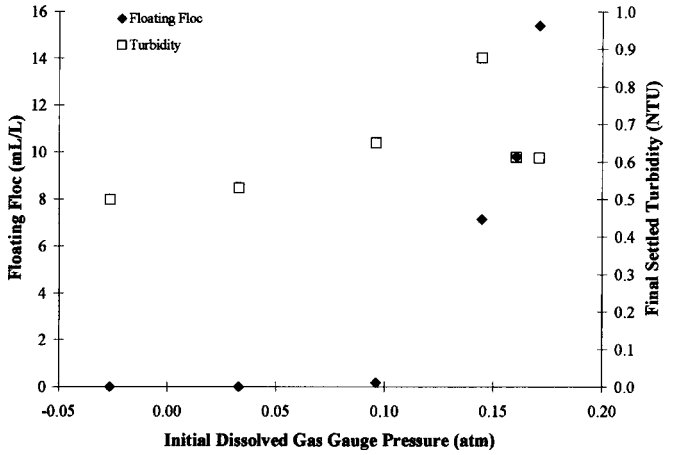

Fig. 7. Change in floating floc and turbidity as a function of initial dissolved gas and alum coagulant [solutions were rapid mixed at 80 rpm ($G=120\ s^{-1}$) for 60 s and flocculated at 5 rpm ($G=2\ s^{-1}$)]

"preexisting" bubbles probably contributed to floating floc, since rapid mixing usually began within a minute of filling the first jar. In an experiment where these bubbles were allowed to leave solution prior to rapid mixing, there was 35% less floating floc than in similar waters that were rapid mixed ($G=120\ s^{-1}$ for 60 s) immediately after filling the jars. It was clear, then, that most bubbles were forming during rapid mixing [Eq. (3)].

Bubble formation can be further characterized dependent on whether the bubbles attached to floc. That is, many of the larger gas bubbles (diameter=1–2 mm) did not attach to coagulant floc and floated quickly to the water surface at the start of slow mixing without major disruptions to flocculation or sedimentation. Smaller gas bubbles (diameter $\leq$0.2 mm) were seemingly held in suspension during the slow mix flocculation and could readily attach to newly formed coagulant floc, and these bubbles often were not visible until after a few minutes of slow mixing.

The bubbles that initially attached to the coagulant floc were observed to have several possible fates:

1. Bubble(s) floated the coagulant floc to the water surface;
2. Some floc settled properly even with bubbles attached;
3. Bubbles on settled floc sometimes continued to grow, causing previously settled floc to resuspend with time;
4. Bubbles detached from the floating floc, allowing the floc to settle; and
5. Bubbles floating to the water surface could disrupt other floating floc, separating previously attached bubbles from the floc.

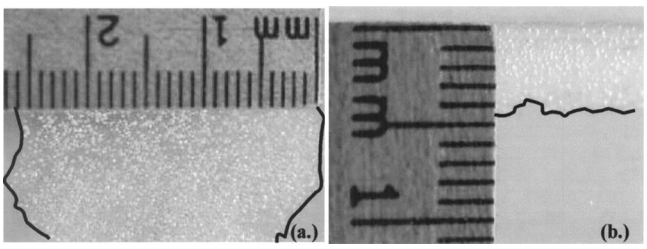

Fig. 8. Quantification of alum floating floc by estimating (a) surface diameter and (b) depth/thickness of the floating floc (black lines added were to accent the outline of the floating floc)

Bubbles were sometimes broken free of the floc by mixing, and more rigorous mixing caused more detachment.

Changes in floating floc volume are therefore a function of factors causing its formation and factors that destroy it:

$$(\partial \text{floating floc})/(\partial \text{time}) = \text{formation} - \text{losses} \tag{4}$$

Conceptually, formation of floating floc is probably described by an equation with the following terms:

$$\text{formation} \approx (\text{bubble concentration})(\text{attachment factors}) \times (\text{floc concentration}) \times (\text{extent of local dissolved gas supersaturation}) \tag{5}$$

That is, without floc or bubbles, floating floc formation is zero. Likewise, if the bubbles and floc are both present but do not attach, then floc cannot be floated. More detailed explanations of these phenomena can be found in the dissolved air floatation literature (Edzwald 1995).

In addition, the surface properties of the coagulant could influence the degree of bubble attachment and nucleation, since a hydrophobic surface typically creates more nucleation sites for bubble formation and is more likely to attach to a preformed bubble than a hydrophilic surface (Harvey 1975). Solid iron hydroxide [$Fe(OH)_{3(s)}$] is often considered more hydrophobic than solid aluminum hydroxide [$Al(OH)_{3(s)}$], which is more hydrated (Edzwald 1995). Since the surface charge of gas bubbles and solid particles can vary significantly depending on properties of the solution, electrostatic forces can also influence bubble attachment to floc.

Losses in floating floc volume are probably described by an equation with the following terms:

$$\text{losses} \approx (G)(\text{volume of floating floc})(\text{attachment factors}) \tag{6}$$

In other words, loss requires the presence of preexisting floating floc volume. Faster mixing (G) will cause detachment, and the strength by which bubbles are held by floc will also play a role.

Consistent with these concepts, typical results at a given mixing speed (160 rpm, $G=335\ s^{-1}$) led to a maximum volume of floating floc at a specified time (Fig. 9). Bubble concentrations were high early in the mixing sequence, so floating floc increased rapidly for a time (Zone 1). At longer mixing times, the volume of floating floc declines (Zone 2), which can be explained by two possibilities: bubble growth continued during rapid mixing with larger bubbles leaving the solution quickly [i.e., low bubble concentration in Eq. (5)] or bubbles attached to floc are detached by continual mixing [Eq. (6)]. Eventually, if mixing times are long enough, no floating floc remains (Zone 3). A sharp peak in floating floc volume was observed at a mixing time of 15 s for this system (0.20 atm gauge pressure, 160 rpm, $G=335\ s^{-1}$). Experiments also demonstrated that bubble attachment to floc may be important and change with time. Specifically, if the water in Fig. 9 was rapid mixed 600 s without coagulant and then coagulant was suddenly dosed with 15 s of additional rapid mixing, 2.9 mL/L floating floc formed. No floating floc was present after this total rapid mix time when coagulant was added at the start, even though the dissolved gas content was the same.

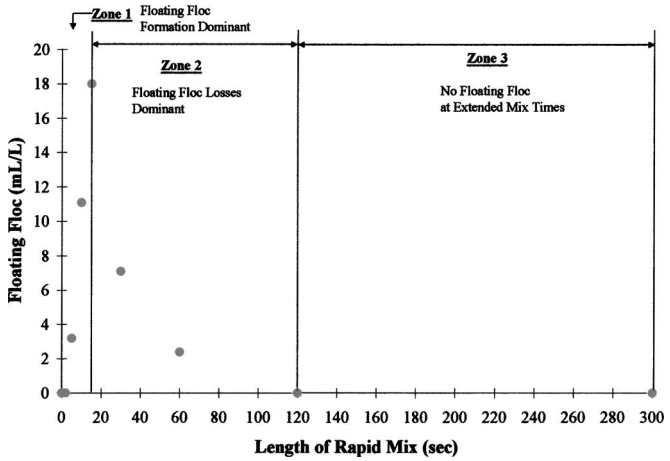

Fig. 9. Variations in floating floc as a function of the rapid mix length [solutions were initially at 0.20 atm gauge pressure, rapid mixed at 160 rpm (G=335 s^{-1}), and flocculated at 5 rpm (G=2 s^{-1})]

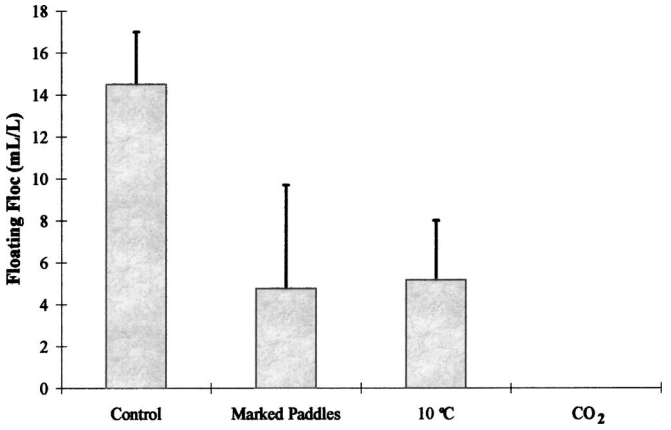

Fig. 11. Factors affecting gas bubble nucleation and floating floc. [Solutions were initially at 0.20 atm gauge pressure, rapid mixed at 80 rpm (G=120 s^{-1}) for 60 s, and flocculated at 5 rpm (G=2 s^{-1}). The control solution was dissolved nitrogen supersaturation at 20°C with an unaltered paddle. The experiments with marked paddles (covered with permanent marker) and at 10°C had dissolved nitrogen supersaturation. Error bars represent 95% confidence.]

Quantitative Results in Relation to Background, Theory, and General Observations

Importance of Surface Nucleation Sites

Experiments tested the effects of altering either the mixing paddle surface or the water quality (by addition of surfactants), while the water was initially supersaturated at 0.20 atm dissolved nitrogen gauge pressure. The amount of bubble formation was observed on the paddle and photographed after 30 min while mixing at 40 rpm (G=42 s^{-1}) (Fig. 10). Each scenario was compared to a control solution with an unaltered paddle and without any surfactants [Fig. 10(a)]. Since regular dishwashing soap appeared to reduce the amount of gas bubble nucleation on the paddle [Fig. 10(b)], further testing examined hexametaphosphate and natural organic matter (NOM) at concentrations close to those applied or present during water treatment. Although NOM (2 mg/L as C) did not seem to significantly change the bubble formation compared to the control [Fig. 10(c)], bubble formation was markedly reduced when hexametaphosphate (3.5 mg/L as P) was present in solution [Fig. 10(d)].

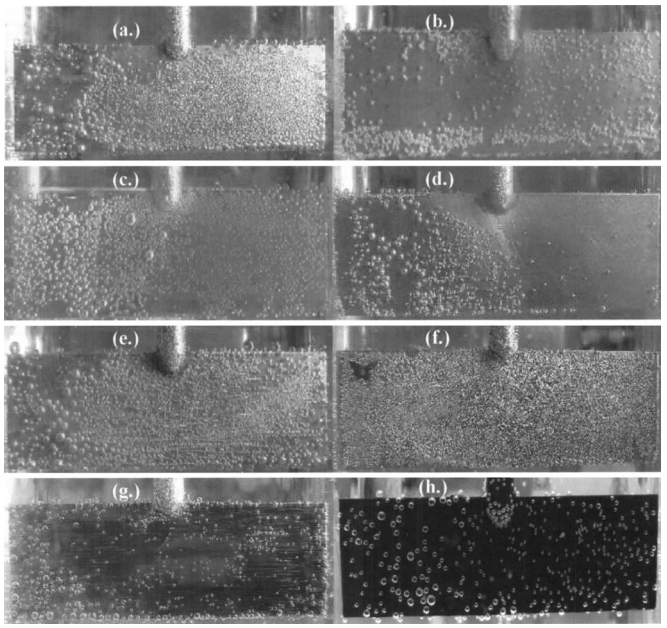

Fig. 10. Visual observations of bubble nucleation on paddle during nucleation experiments: (a) control; (b) dish soap; (c) NOM; (d) hexametaphosphate; (e) sandpaper; (f) fine polish; (g) permanent marker; and (h) paint [solutions were mixed at 40 rpm (G=42 s^{-1}); painting the surface could smooth surface imperfections that cause gas bubble nucleation or could make the surface more hydrophobic]

Bubble nucleation was not significantly enhanced by roughing the paddle with coarse sandpaper [Fig. 10(e)], yet polishing the paddle with a smooth grinder did change the nature of nucleation, creating many gas bubbles with much smaller diameters than the control [Fig. 10(f)]. In this test, interestingly, no bubbles were noted on a colored mark that was used to designate the polished side [Fig. 10(f)]. When a regular paddle was completely marked with the same permanent marker, the amount of bubble formation was greatly reduced [Fig. 10(g)]. Similar results occurred with a completely painted paddle [Fig. 10(h)]. Although the marker and paint most likely made the surface more hydrophobic, smooth hydrophobic surface produces little bubble formation (Ryan and Hemmingsen 1993), so it is also possible that the marker/paint smoothed surface imperfections and reduced the number of nucleation sites.

If a modified, painted paddle surface caused a reduction in gas bubble nucleation, would this then lead to less floating floc in a jar test? To test this hypothesis, jar tests were conducted with waters that were supersaturated initially at 0.20 atm gauge pressure, rapid mixed at 80 rpm (G=120 s^{-1}) for 60 s, and flocculated at 5 rpm (G=2 s^{-1}). When the paddles were completely painted/marked with the permanent marker, the amount of floating floc was less (4.8 mL/L) than in control experiments with unmodified paddles (14.5 mL/L)—a result significant at greater than 95% confidence (Fig. 11). The net conclusion is that for systems where bubble formation occurs on the mixing paddle, painting or replacement with a different paddle material could greatly decrease the amount of bubble formation and floating floc.

Since the number and type of nucleation sites appeared to influence the amount of floating floc, it was anticipated that other

sources of nucleation sites such as bentonite clay might also increase bubble formation. In another jar test with unmodified paddles, the waters initially had 0.20 atm gauge pressure and 10 NTU of bentonite clay turbidity. There was no statistical increase of floating floc in the turbid waters compared to control solutions with no initial turbidity (data not shown). Thus, the paddle type and surface exerted a primary controlling influence in these experiments.

Type of Dissolved Gas Supersaturation

Waters supersaturated with dissolved carbon dioxide (0.20 atm gauge pressure) were compared to solutions supersaturated with dissolved nitrogen (0.20 atm gauge pressure). No floating floc resulted in solutions supersaturated with dissolved carbon dioxide (Fig. 11), which was surprising given the previous predictions regarding faster mass transfer and greater bubble volumes at equilibrium with carbon dioxide (Table 1). The acid-base chemical reactions of carbon dioxide and carbonate species (H_2CO_3, HCO_3^-, CO_3^{-2}) can affect mass transfer kinetics (Howe and Lawler 1989), which is primarily a result of corresponding pH changes. In these experiments, a significant buffering alkalinity still existed at the experimental coagulation pH 6, such that observed pH changes during the course of the jar test were negligible with respect to the abundance of measured dissolved gas supersaturation. Furthermore, the presence of carbonic acid (H_2CO_3) was also insignificant, since at pH 6 the relative equilibrium amount of carbon dioxide was 99.8% (0.2% H_2CO_3). Consequently, any effects from acid-base reactions were deemed negligible in these jar test experiments.

Extensive follow up experiments sought to explain the lack of floating floc during carbon dioxide supersaturation. Considering the possibility that higher ionic strength in the carbon dioxide solution affected floating floc development, solutions supersaturated with nitrogen at the equivalent higher ionic strength (0.029 M) were tested and actually had an increase in floating floc. In addition, zeta potential measurements of many different solutions showed that electrostatic forces did not control this phenomenon.

The higher mass transfer rate caused by the carbon dioxide supersaturation appeared to affect the formation and stability of floating floc in these solutions (Table 1). During and immediately after rapid mixing, gas bubbles in the carbon dioxide waters appeared to be larger ($\approx$0.33 mm diameter) than bubbles in the nitrogen solutions ($\approx$0.20 mm diameter), as measured from still photographs containing a reference scale. The corresponding rise velocity of these bubbles calculated using Stoke's law for spheres ($\rho_b = 1.20$ kg/m^3 at 20°C) would be 6.0 and 2.2 cm/s, respectively, so perhaps it is not surprising that many of the bubbles in the carbon dioxide solutions floated quickly to the water surface without attaching to any coagulant floc. In terms of Eq. (5), the larger bubbles that formed in the presence of carbon dioxide represented an overall lower concentration in the number of bubbles and had a lower tendency to attach to floc.

Some bubbles that remained in the carbon dioxide solutions (diameter $\leq$0.20 mm) did cause floating floc initially. Yet, these newly formed floating floc were disrupted by bubble growth that steadily continued on the paddle or walls of the jar. When these bubbles (1–2 mm diameter) floated quickly to the water surface, some of the new formed floating floc was agitated, separating previously attached bubbles from the coagulant floc [Eq. (6)]. For example, the amount of floating floc in one carbon dioxide jar test was 0.7 mL/L at the end of flocculation, but only 0.02 mL/L of floating floc remained following the 30 minutes of settling (Fig. 11). This agitation caused by other gas bubbles was not normally observed in solutions supersaturated with only dissolved nitrogen but did occur in waters with dissolved nitrogen and carbon dioxide both at 0.10 atm gauge pressure (0.20 atm total gauge pressure) (Table 1).

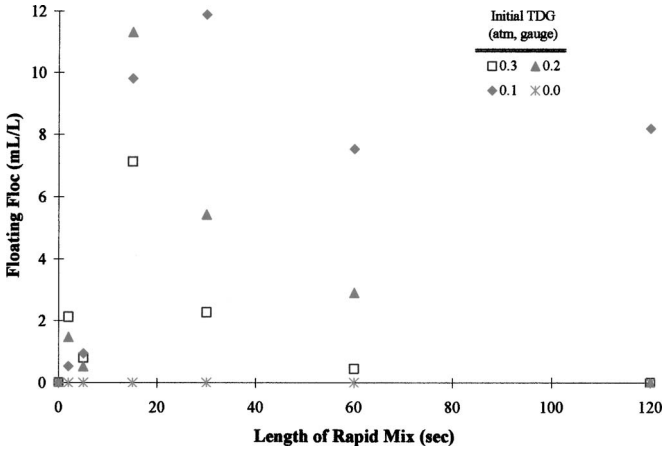

Fig. 12. Floating floc as a function of initial TDG and length of rapid mixing [solutions were rapid mixed at 160 rpm ($G = 335$ s^{-1}) for 60 s, and flocculated at 5 rpm ($G = 2$ s^{-1})]

Similar mass transfer observations have been documented previously in experiments that monitored size changes of a preformed bubble exposed to oscillatory pressure variations. With "air" present as the dissolved gas, the size of the bubble seemed insensitive to mass transfer even during times of dissolved gas supersaturation (Ran and Katz 1991). Yet, during similar experiments with carbon dioxide dissolved in solution, significant bubble size changes were observed, with varying rates of mass transfer of carbon dioxide (Ran and Katz 1991).

In summary, bubble formation and floating floc varied depended on the type of dissolved gas supersaturation. In these experiments, dissolved carbon dioxide supersaturation seemed to produce more overall bubble formation but also less floating floc. These results were not anticipated and should be investigated further.

Dissolved Gas Supersaturation and Floating Floc

In a preliminary experiment, the amount of floating floc seemed to increase with the initial dissolved gas supersaturation, consistent with the initial idea that higher mass transfer and bubble formation would then lead to more floating floc (Fig. 7). Consequently, most experiments were designed with water initially supersaturated at 0.20 atm gauge pressure. Yet, given the surprising results for the carbon dioxide jar tests, additional experiments considered other levels of dissolved nitrogen supersaturation (0.00–0.30 atm gauge pressure) for a range of rapid mix lengths [0–120 s at 160 rpm ($G = 335$ s^{-1})].

Except for one experiment at 2 s of rapid mixing, waters with the highest initial dissolved gas supersaturation tested (0.30 atm gauge pressure) had less floating floc than all other solutions (Fig. 12). Extensive bubble formation was observed in these solutions, and continued throughout slow mix flocculation. Yet bubbles floating to the water surface broke apart newly formed floating floc as observed in the previous experiment with carbon dioxide supersaturation. This phenomenon did not seem to impact solutions tested at lower initial dissolved nitrogen supersaturation. The implication is that there is a level of supersaturation where

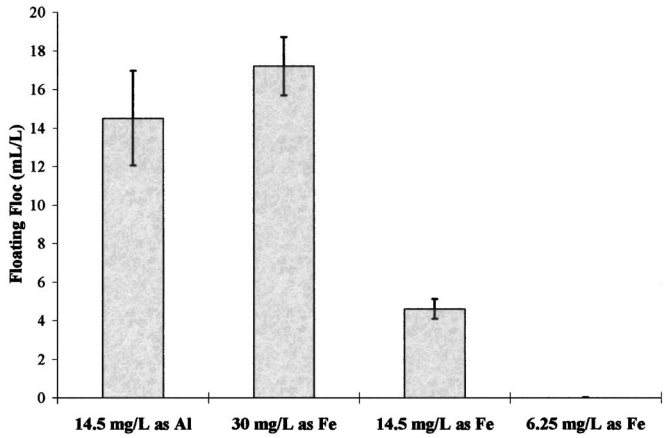

Fig. 13. Comparison of alum and iron(III) chloride coagulants. [Solutions were rapid mixed at 80 rpm ($G=120\ s^{-1}$) for 60 s and flocculated at 5 rpm ($G=2\ s^{-1}$). Error bars represent 95% confidence.]

Table 2. Comparison of the Amirtharajah and Mills (1982) and This Study

Aluminum dose (mg/L as $Al_2(SO_4)_3 \cdot 16H_2O$)	pH	Equilibrium bubble formation[a] (mL/L)	Initial turbidity (NTU)	Settled turbidity[b] (30 min) $G=300\ s^{-1}$	Settled turbidity[b] (30 min) $G=16,000\ s^{-1}$
Amirtharajah and Mills (1982)					
5	5.85	1.07	—	24	18
1	6.45	0.79	—	17	18
30	6.45	0.79	—	16	3
This study					
5	5.95	1.03	22.4	24	—
5	5.90	1.05	18.3	—	22

[a]Calculated with the Modified Closed System Model (Scardina and Edwards 2001).

[b]No floating floc was observed in these experiments.

any additional dissolved gas actually decreases the occurrence of floating floc. Also, the worst rapid mix time was 15 s at 0.20 or 0.30 atm gauge pressure but was 30 s at 0.10 atm gauge pressure. At 0.10 atm gauge pressure, 120 s of rapid mixing did not decrease floating floc; whereas, at 0.20 and 0.30 atm gauge pressure, 120 s rapid mixing virtually eliminated such problems.

Effects of Solution Temperature

Solutions supersaturated with 0.20 atm gauge pressure nitrogen at 10°C were compared to similar solutions but at 20°C. The measured floating floc in the 10°C waters was significantly less than what formed in the 20°C system (Fig. 11). As predicted previously, the lower diffusion rate at 10°C (Table 1) probably reduced overall mass transfer, causing less total bubble formation and corresponding floating floc. Even though colder solutions were less susceptible to floating floc in these experiments, any warming of a colder water within a treatment plant would increase the dissolved gas pressure, and could increase the potential for bubble formation and floating floc.

Effects of Coagulant Type

The same alum dose (14.5 mg/L as Al) was used throughout this study, and for a comprehensive comparison, three iron concentrations were tested, equivalent to the molar (30 mg/L as Fe) and mass (14.5 mg/L as Fe) concentrations of the aluminum. Since iron and aluminum hydroxides can precipitate quite differently even at similar molar concentrations, a third iron dosage (6.25 mg/L as Fe) was visually selected from an iterative experiment in water undersaturated with dissolved gas to replicate the approximate floc size/volume observed for aluminum. All solutions were rapid mixed at 80 rpm ($G=120\ s^{-1}$) for 60 s and flocculation at 5 rpm ($G=2\ s^{-1}$).

At the equivalent molar concentration (30 mg/L as Fe), the iron flocs appeared to form instantaneously but became much larger and more abundant. As a consequence, these larger flocs seemed to have more gas bubbles attached, resulting in a comparable volume of floating floc relative to aluminum (Fig. 13). In contrast, in the same experiment with solutions undersaturated with dissolved gas, most of these iron flocs settled naturally during the flocculation stage. The total amount of floating floc decreased at the lower iron dosages (Fig. 13); therefore, in these particular experiments, larger floc particles and higher coagulant doses did not improve settling efficiency but actually worsened floating floc.

Two additional observations are deemed noteworthy. First, at the lowest iron dose (6.25 mg/L as Fe), the coagulant flocs did not become visible until after 15 min of slow flocculation. At this point the vast majority of bubbles that formed during rapid mixing had naturally escaped to the water surface, such that there was almost no floating floc in this experiment due to a low number of available bubbles [Eq. (5)]. Slow appearance of visible floc also occurred in the study by Amirtharajah and Mills (1982). Although calculations indicate that certain waters in that study were likely supersaturated with dissolved gas, when we repeated their experiments, there was no observed floating floc (Table 2).

The second anomaly of interest occurred in the solutions undersaturated with dissolved gas and coagulated at 30 mg/L as Fe. Although no gas bubbles formed in these waters, some of the coagulant naturally floated at the water surface. No other floating floc appeared in any other experiments when the water was undersaturated with dissolved gas. The cause of this floating floc was not determined, but it might be an indication of the inherent hydrophobicity of precipitated iron hydroxide. This floating floc was of little consequence, since the vast majority of floc settled properly, but it does warrant further investigation.

Even if iron hydroxide precipitates are more hydrophobic in waters prone to bubble formation, floating floc could result with either aluminum or iron coagulants (Fig. 13). The type of coagulant did not seem to control the problem.

Effects of High Rate Mixers

Very high rate mixers are sometimes appealing to utilities for instantaneous chemical dispersal and have been found in some cases to be beneficial (Amirtharajah and Mills 1982). Some experiments were conducted with rapid mix speeds of 1,300 and 2,200 rpm (7,775 and 17,120 s^{-1}, respectively), and as noted previously, mixing at these speeds induced negative local gauge pressures [Fig. 6 (bottom)]. Bubbles were scattered throughout solution following both high rate mixes, even in waters initially undersaturated with dissolved gas relative to the atmosphere. However, even though bubbles were readily produced by the high rate mixers, floating floc did not develop in solutions with no

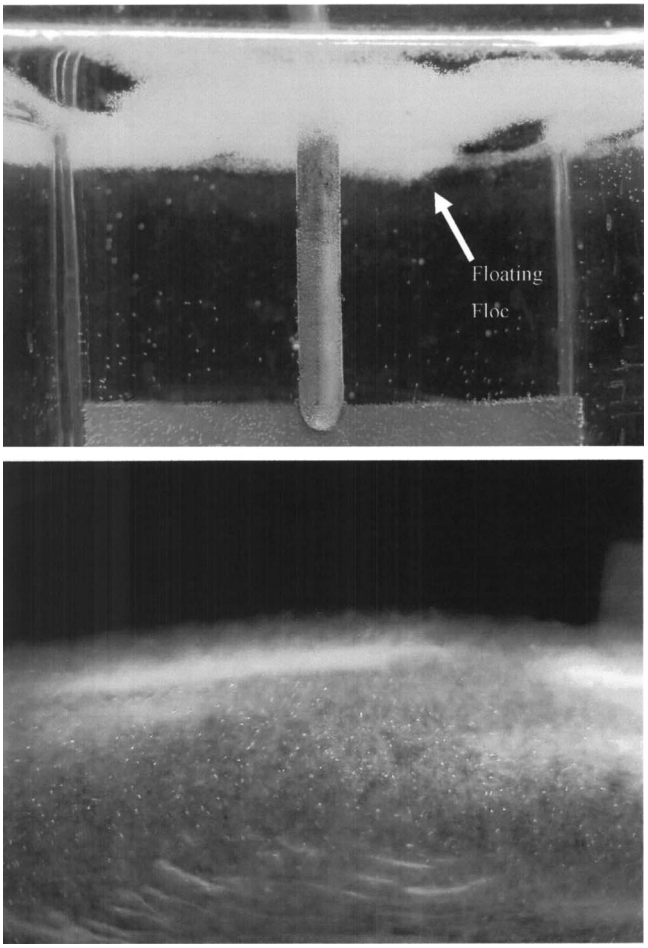

Fig. 14. High rate mixing experiments at 1,300 rpm. (top) Floating floc in waters rapid mixed for 2 s and (bottom) bubbles enmeshed in settled floc rapid mixed at 10 s.

(0.00 atm gauge pressure) or very little dissolved gas supersaturation (0.03 atm gauge pressure). Many bubbles were indeed attached to the coagulant floc, but without a sufficient driving force of dissolved gas supersaturation, bubbles did not grow enough to buoy the floc.

In waters supersaturated at 0.20 atm gauge pressure nitrogen subjected to high rate rapid mixing, floating floc was again dependent on the time length of rapid mixing. For example, essentially all of the coagulant floc was floated to the water surface in solutions with short rapid mix times (1–5 s) [Fig. 14 (top)], whereas most all of the floc settled in waters with longer mixing times (10–15 s) [Fig. 14 (bottom)]. Unlike the previous experiments where settling improved at longer rapid mix times (Figs. 9 and 12), bubbles were enmeshed in these settled floc [Fig. 14 (bottom)], which was consistent at both high rate mixing speeds. Upon closer visual inspection, there appeared to be a difference between the coagulant flocs, such that flocs from shorter rapid mixes seemed to be much "fluffier" and less dense. Slight differences in pH were not the cause of these phenomena, since similar results occurred in solutions carefully maintained at pH 6. As observed in the Amirtharajah and Mills study (1982), how the water is rapid mixed can effect the corresponding precipitated coagulant floc. The inherent creation of denser floc may be less susceptible to floating in the presence of bubbles.

Additional Considerations

As apparent in the high rate mixer experiments, the presence of gas bubbles could have affected the mass density of newly precipitated coagulant floc. Obviously, if the presence of gas bubbles influenced formation of a less dense coagulant floc, then the overall effects of bubble formation would be compounded. As a first approximation in this work, the coagulant floc density was assumed to be constant for all experiments, such that any density variations were considered negligible in floating floc calculated volumes. Future studies should consider changes in the density of coagulant floc when gas bubble formation is also present.

Other system properties might also influence bubble formation and floating floc. For example, any entity absorbed onto a coagulant could change the overall surface properties of the floc, such as NOM. Even though NOM did not markedly affect bubble formation on the mixing paddle (Fig. 10), NOM could change the surface charge (electrostatic forces) and make the surface more hydrophobic (hydrophobic forces). Ionic strength, acid-base properties of the surface, and the bubble surface charge could also affect bubble-floc attachment forces. Further analysis should systematically investigate surface chemistry interactions of the bubble and floc for conditions common in drinking water treatment.

Summary and Conclusions

- Bubbles attached to coagulant floc can cause floatation, which reduces settling and particle removal efficiency. Both aluminum and iron coagulants are susceptible to this problem.
- For waters supersaturated with dissolved gas, a rapid mix paddle can be a location of minimum pressure in the system and a source of bubble formation. If the local solution pressure during rapid mixing estimated by the energy equation is less than the measured total dissolved gas pressure, then bubbles can form. Painting the paddle surface could reduce the amount of bubble formation by smoothing surface imperfections that serve as nucleation sites for bubble formation.
- Very high rate rapid mixers can cause bubble formation, even in a water undersaturated with dissolved gas relative to the atmosphere.
- Many system properties control the formation and stability of floating floc including the local solution pressure, amount and type of dissolved gas supersaturation, temperature, and the duration of rapid mixing. The exact response is likely to be system specific but are likely to follow general trends outlined herein.
- Dissolved gas supersaturation and bubble formation should be considered in the design of coagulation/sedimentation systems. The results presented can be a tool to mitigate floating floc.

Acknowledgments

This work was supported by the American Water Works Association Research Foundation (AWWARF) under Grant No. 2821. The opinions, findings, conclusions, or recommendations are those of the writers and do not necessarily reflect the views of AWWARF. Many of these experiments were performed by Kenneth Craft Jr. as undergraduate research. His efforts are greatly appreciated.

References

Amirtharajah, A., and Mills, K. M. (1982). "Rapid mix design for mechanisms of alum coagulation." *J. Am. Water Works Assoc.*, 74(4), 210.

Betterton, E. A. (1992). "Henry's law constants of soluble and moderately soluble organic gases: Effects on aqueous phase chemistry." *Gaseous pollutants: Characterization and cycling*, J. O. Nriagu, ed., Wiley, New York.

Birkhoff, G. (1957). *Jets, wakes, and cavities*, Academic, New York.

Droste, R. L. (1997). *Theory and practice of water and wastewater treatment*, Wiley, New York, 389–394.

Edzwald, J. K. (1995). "Principles and applications of dissolved air flotation." *Water Sci. Technol.*, 31(3), 1.

HACH Co. (1997). *HACH model 2100N laboratory turbidimeter instruction manual*.

Harvey, H. H. (1975). "Gas disease in fishes—A review." *Proc., Chemistry and Physics of Aqueous Gas Solutions, Electrothermics and Metallurgy and Industrial Electrolytic Divisions*, The Electrochemical Society, Princeton, N.J., 450–485.

Hayduk, W., and Laudie, H. (1974). "Vinyl chloride gas compressibility and solubility in water and aqueous potassium laurate solutions." *J. Chem. Eng. Data*, 19(3), 253.

Hilton, A. M., Hey, M. J., and Bee, R. D. (1993). "Nucleation and growth of carbon dioxide gas bubbles." *Food colloids and polymers: Stability and mechanical properties, special publication 113*, Royal Society of Chemistry, Cambridge, U.K., 365–375.

Howe, K. J., and Lawler, D. F. (1989). "Acid-base reactions in gas transfer: A mathematical approach." *J. Am. Water Works Assoc.*, 81(1), 61–66.

Letterman, R., and Shankar, S. (1996). "Modeling pH in water treatment plants: The effect of carbon dioxide transport on pH profiles." *Poster at the 1996 AWWA National Conf.*, Toronto.

Ran, B., and Katz, J. (1991). "The response of microscopic bubbles to sudden changes in the ambient pressure." *J. Fluid Mech.*, 224, 91–115.

Robertson, J. A., and Crowe, C. T. (1993). *Engineering fluid mechanics*, 5th Ed., Houghton Mifflin Company, Boston.

Ryan, W. L., and Hemmingsen, E. A. (1993). "Bubble formation in water at smooth hydrophobic surfaces." *J. Colloid Interface Sci.*, 157, 312–317.

Ryan, W. L., and Hemmingsen, E. A. (1998). "Bubble formation at porous hydrophobic surfaces." *J. Colloid Interface Sci.*, 197, 101–107.

Sander, R. (1999). "Compilation of Henry's law constants for inorganic and organic species of potential importance in environmental chemistry—Version 3." ⟨http://wee.Mpch-main2mpg.de/~sander/res/henry.html⟩.

Scardina, P. (2004). "Effects of dissolved gas supersaturation and bubble formation on water treatment plant performance." Ph.D. dissertation, Virginia Tech., Blacksburg, Va.

Scardina, P., and Edwards, M. (2001). "Prediction and measurement of bubble formation in water treatment." *J. Environ. Eng.*, 127(11), 968–973.

Scardina, P., and Edwards, M. (2002). "Practical implications of bubble formation in conventional treatment." *J. Am. Water Works Assoc.*, 94(8), 85.

Selleck, R. E., Mariñas, B. J., and Diyamandoglu, V. (1988). "Treatment of water contaminants with aeration in counterflow packed towers: Theory, practice, and economics." *UCB/SEEHRL Rep. No. 88-3/1*, Univ. of California, Berkeley, Calif.

Van't Riet, K., and Smith, J. M. (1975). "The trailing vortex system produced by rushton turbine agitators." *Chem. Eng. Sci.*, 30, 1093–1105.